Jurnal Teknologi

Full Paper

FLEXIBLE DYNAMIC MODEL OF ATTITUDE MANEUVERING OF RAZAKSAT® SATELLITE

Teoh Vil Cherd*, Shahriman Abu Bakar, Sazali Yaacob, Nor Hazadura Hamzah

School of Mechatronic Engineering, Universiti Malaysia Perlis, Perlis, Malaysia

Article history
Received
1 June 2015
Received in revised form
13 July 2015
Accepted
20 August 2015

*Corresponding author
Vaticano87@gmail.com

Graphical abstract

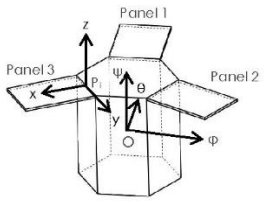

Abstract

In this paper, a dynamic model equation of the RazakSAT® class satellite three flexible solar panels for three-dimensional dynamic studies is developed based on the coupling deformation field. In the model, each solar panel is flexible and attached to the satellite body via a fixed joint where the assumption of Euler-Bernoulli beam is applied for the solar panels. Lagrange and assumed mode method are used to develop the dynamic model of the RazakSAT® multi-body system. A comprehensive model of flexible satellite has been provided in ANSYS environment as a reference when simulating the theoretical response generated by MATLAB to show that the coupling effect on the characteristics of the flexible sub system while undergoing rigid-body rotational motion.

Keywords: RazakSAT, flexible, satellite

Abstrak

Kertas kerja ini, persamaan model dinamik kelas RazakSAT® satelit dengan tiga panel solar fleksibel untuk tiga dimensi dihasilkan berdasarkan gandingan ubah bentuk objek. Model tersebut memaparkan sifat-sifat panel solar yang fleksibel dan dipasangkan pada badan satelit dengan sendi tetap di mana andaian Euler-Bernoulli diaplikasikan pada ciri-ciri fleksibel panel solar. Kaedah Lagrange dan "Assumed Mode Method" digunakan untuk menghasilkan model dinamik sistem serba badan RazakSAT®. Perisian ANSYS digunakan untuk menghasilkan data-data getaran panel solar yang akan digunakan sebagai rujukan terhadap kesimpulan daripada simulasi yang dijana oleh oleh MATLAB semasa badan satelit menjalani putaran pada pusat gravity jasad satelit.

Kata kunci: RazakSAT, flesibel, satellit

1.0 INTRODUCTION

Responding to the ever increasing demand of complexity of space mission, modern day spacecraft are often designed to carry deployable appendages such as the solar panels, booms or antennas, which are flexible in nature. The development of model of rotating multi-body systems have been done mainly for the design of satellite attitude control where by understanding of the attitude behavior becomes a priority and is performed via numerical analysis and computer simulation [1]. The satellite mathematic model included the interaction between the rigid structures and flexible components. Establishment of the model is a difficult task to accomplish due to the involvement of complex dynamics characterized by nonlinearities and strong coupling between flexible and rigid modes which is pointed out in [2], the increasing size, flexibility, and dynamic complexity, coupled with competing demands for greater precision and autonomy, continue to hinder our ability to model these systems sufficiently. In addition to that, the modern engineering technology is leading to more demanding operational requirement, such as

high speed rotation and large angular motion, great precision and pointing accuracy, which have posed serious difficulties for all currently advocated control design methodologies [3].

Researchers in paper [4-9] have confined the research on the boundary of planar motion of a satellite body and rotation about the normal axis. Study on planar motion is crucial as it helps overcome most of the obstacles in modeling of a three-dimensional motion model, which facilitates the use of simple models, such as the Euler-Bernoulli beam, and mode summation procedure. The planar model and mode summation procedure have been commonly used in developing a flexible satellite model for adaptive control [4] and control design based on the Lyapunov stability theory [5]. Publication [6] had touched on the application of active control method to reduce vibration in the planar motion via a piezoelectric and is determined by using the Euler-Bernoulli model. Vibration control on a planar model is illustrated in [7]. In order to simulate the vibration of solar panels, the mode summation procedure is used in [7]. The dynamic model of the satellite can be obtained from a real satellite or laboratory setup [8-9]. In [8], experiment of an attitude control of a satellite with an L-shaped appendage was done in a laboratory setup. The control motion of the satellite was planar, and the L-shaped appendage in the plane with the rotational motion. The measurement and control of the vibratory motion of the flexible appendage is done by attaching infrared sensors and a piezoceramic actuator to the L-shaped appendage [9].

RazakSAT® has applied the rigid model as the key model in the controller design. However, in the case of high-speed and long range motion, the protruding solar panels would produce the flexible phenomena due to the elastic deflection, and traditional rigid dynamic analysis can hardly deal with this phenomenon. Traditional modeling adopts small deformation assumption in structural dynamics, which assumes that the transverse deformations at any point in the beam are negligible. In this paper, a dynamic equation of a RazakSAT® class satellite three flexible solar panels for three-dimensional dynamic studies is developed based on the coupling deformation field. Normal planar environment is unable to accommodate the dynamics of RazakSAT® due to the nature of the design whereby the panels are appended on an angle to the principle axis. Compared with finite element method utilized in the references [10, 12] for studying the dynamic characteristic, the assumed mode method adopted here has the property of simplicity, especially applicable to controller design.

2.0 FLEXIBLE MODEL

RazakSAT® is composed of a multi-body configuration of a rigid body appended with three flexible solar panels. The satellite executes flexible behavior contributed by the vibratory motion of the solar panels. The nature of the fix-free arrangement joint of the solar panels is idealized into cantilever beams, and is subjects to rotational and vibrational motion. The presence of flexible behavior in the dynamics makes the basic Newton Law undesirable. Hence, the "Rayleigh-Ritz Assumed Mode Method", is applied instead to obtain the model. Unlike the rigid model derived in section 2, it initiates with the expression of the total energy of the satellite system which comprised of both kinetics and potential energy. The schematic diagram of RazakSAT® satellite's rigid hub and the three elastic appendages is illustrated in Figure 1. The three solar panels appended on the rigid hub are given the notation of 1 to 3 as shown in Figure 1. The global Cartesian axis is based on the principle axis of the satellite is whereby the torque is applied along it and is termed Roll (φ), Pitch (θ) and Yaw (ψ). In the case of RazakSAT®, the torque is generated by four unit of reaction wheels which are configured in a *tetrahedron* array. The local axes of the solar panel are denominated as x, y and z and is located at point $O_i'(a_i, b_i, c_i)$.

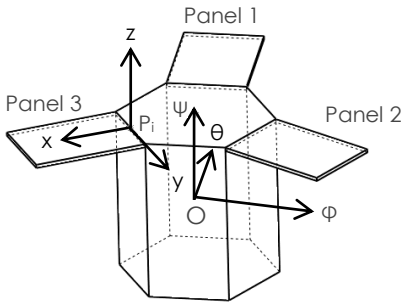

Figure 1 RazakSAT® diagram

The total energy of the system equates to the summation of the total kinetic and potential energy. Kinetic Energy, T may be obtained as described in (1), whereby I is the moment of inertia of the rigid center hub of the satellite, $\dot{\theta}$ is the angular speed of the satellite body, while, ρ_i and $\bar{V}_i$ is the mass per unit volume of solar panel, and velocity of unit mass of the appendage respectively. These variables are embodied with the notation i which will represent the identity of each panel present in the satellite model where in RazakSAT® case, i=1 to 3.

$$\frac{1}{2}\left\{I\dot{\theta}^2 + \sum_{i=1}^{3} \rho_i \left[\int_0^{z_i}\int_{-\frac{w_i}{2}}^{\frac{w_{i1}}{2}}\int_0^{L_i} \bar{\mathbf{V}}_\mathbf{i}\cdot\bar{\mathbf{V}}_\mathbf{i}\,dxdydz\right]\right\} = \mathbf{T} \qquad (1)$$

The matrix $\bar{V}_i$ is obtained as in (2).

$$\bar{V}_i = \begin{bmatrix} \bar{V}_{\varphi i} \\ \bar{V}_{\theta i} \\ \bar{V}_{\psi i} \end{bmatrix} = [F_i] \cdot \begin{bmatrix} \bar{\varphi} \times R_{ai} \\ \bar{\theta}_y \times R_{bi} \\ \bar{\psi}_z \times R_{ci} \end{bmatrix} + \begin{bmatrix} 0 \\ \dot{u}_i \\ 0 \end{bmatrix} \quad (2)$$

Where variable $\dot{u}_i$ represents the lateral elastic displacement of the solar panel with time t and distance x measured from the point O_i'. Assuming that the deflection is small, notation $\dot{u}_i$ may be expressed in (3).

$$u_i = z_{i,u} k \quad (3)$$

Based on the Euler-Bemouli assumption, the potential energy of the system is

$$U = \sum_{i=1}^{3} \int_0^{L_i} E_i I_i \ddot{z}_{i,u}{}^2 dx \quad (4)$$

Where, $E_i I_i$ is the uniform flexural rigidity of the appendage, and $\ddot{z}_{i,u}$ is the second partial derivative of $z_{i,u}$ with respect to x_i.

2.1 Transformation Matrices

The non-parallel alignment of the local axes of the solar panels to the global axis is required to be tended to prior to the development of the dynamic model. Introduction of sets of matrices termed "translational matrix" is crucial to give the sense of relation between the local and the global axis for it has major implication in the final mathematical model. Illustration in Figure 2 depicts the φ - θ plane of the satellite. Observable from Figure 2, solar panels 1 to 3 are configured with 90, -30 and 210 degree respectively. The transformation matrices are as shown in (5) – (7).

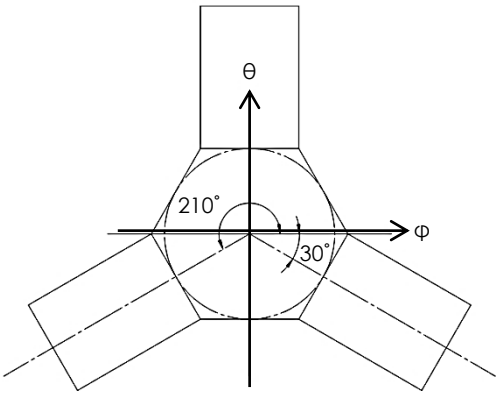

Figure 2 φ - θ plane

$$\text{Appendage } 1, F_1 = \begin{bmatrix} 0 & 1 & 0 \\ 1 & 0 & 0 \\ 0 & 0 & 1 \end{bmatrix} \quad (5)$$

$$\text{Appendage } 2, F_2 = \begin{bmatrix} \cos(-30^\circ) & \sin(-30^\circ) & 0 \\ -\sin(-30^\circ) & \cos(-30^\circ) & 0 \\ 0 & 0 & 1 \end{bmatrix} \quad (6)$$

$$\text{Appendage } 3, F_3 = \begin{bmatrix} \cos(210^\circ) & \sin(210^\circ) & 0 \\ -\sin(210^\circ) & \cos(210^\circ) & 0 \\ 0 & 0 & 1 \end{bmatrix} \quad (7)$$

2.1 Identifying Vector Position

The vector position, R describes the relative position of the point mass along the flexible component of the satellite (Solar Panel) towards the center of the point of executed rotation. The vector position for each axis is shown in section 1 to 3.

2.1.1 Local Panel y-z Plane

Assume that the rotation of the satellite is orthogonal to the plane of y-z as shown in Figure 3. Rotation in this manner is parallel to the local x axis of the panel. The vector position due to this axis of rotation, R_{ai} is given by the (8). The variable c defines vertical offset of the panel from the center of rotation and y_i is the horizontal distance along the panel while z_i represent the vertical distance z axis along of the panel.

$$R_{ai} = (y_i)j + (c + z_i + u_i)k \qquad i = 1,2,3 \quad (8)$$

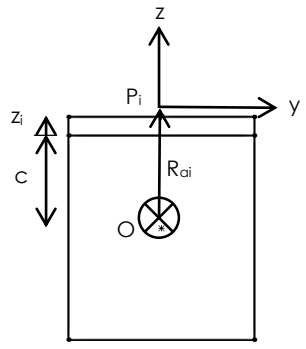

Figure 3 y-z plane

2.1.2 Local Panel x-z Plane

Plane x-z of the solar panel of the satellite is as shown in Figure 4. The variable 'a' represents the horizontal distance between the center of rotation of the satellite to the appending edge of the solar panel. Parameter "x_i" represents the position of a measured point mass element with reference to the edge of the rigid hub along solar panel's x axis. Vector position R_{bi} gives the vector position of the point on the appendage relative to the axis of rotation. The vector of vertical elastic displacement (elastic deformation) measured perpendicular to the axis x is represented

by u_i and the point mass of the solar panel along the z axis is termed z_i. Therefore, the vector position R_{bi} is given by

$$R_{bi} = (a + x_i)i + (c + z_i + u_i)k \qquad i = 1,2,3 \qquad (9)$$

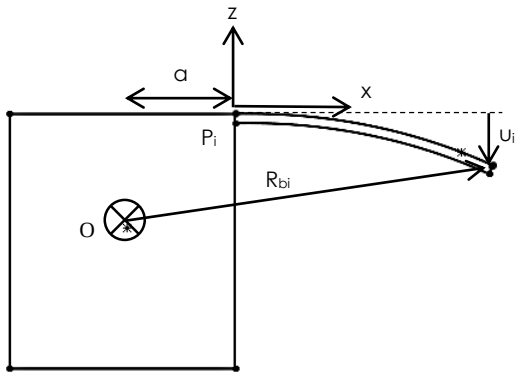

Figure 4 x-z plane

2.1.3 Local Panel x-y Plane

The vector position R_{ci} is derived from Figure 5 which depicts the local x-y plane of one of the solar. In z axis rotation, the panels execute negligible flexible behavior. Hence, R_{ci}, the vector position of any point in the appendage form relative to the body reference is as shown in (10). The vector "x_i" represents the position of a measured mass element along solar panel's x_i axis.

$$R_{ci} = (a + x_i)i + (y_i)j \qquad i = 1,2,3 \qquad (10)$$

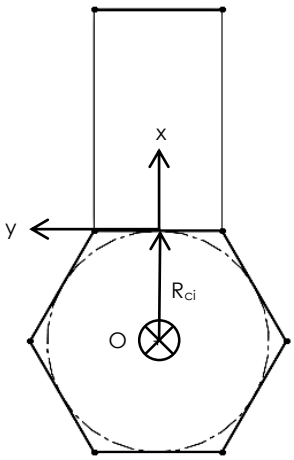

Figure 5 x-y plane

Obtained vector position of the 3 local axes, (8) – (10) are required to obtain the dynamics of the system which present in energy equation of (1) – (4). Section C contains details of the proceeding derivation, initiated by assuming that only φ axis is being applied with torque.

2.2 Energy Equations

Obtaining the total energy equation with respect to φ torque application involves the kinetic and the potential energy. To obtain the kinetic energy due to the torque, substitute (2) – (10) into (1), and leads to (11). The variable D is the angle of appending of the panels which are 90, -30 and 210 for i = 1, 2 and 3 respectively.

$$2T_\varphi = I\dot{\varphi}^2 + \int_0^{z_i}\int_{-\frac{w_i}{2}}^{\frac{w_{i1}}{2}}\int_0^{L_i}\sum_{i=1}^{3}\rho_i[A]dxdydz \qquad (11)$$

Where,

$$A = \begin{bmatrix} \dot{\varphi}^2(c + z_i + z_{i,u})^2 \\ +\{y_i\dot{\varphi}\cos(D_i) + z_{i,u} - (a + x)\dot{\varphi}\sin(D_i)\}^2 \end{bmatrix} \qquad (12)$$

2.3 Discretization

A new assumed equation as in (13) is introduced in order to discretize the energy equation. The lateral displacement, $z_{i,u}$ at any point on the solar panel is the product of a mode shape function, and a harmonic time function:

$$z_{i,u}(x,t) = \sum_{i=1}^{n} q_i(t)\emptyset_i(x) \qquad (13)$$

Variable $\emptyset_i(x)$ is the mode shape, while $q_i(t)$ is the modal generalized coordinate for the i-th mode, and n denotes the number of modes included in the approximation. The mode shape function for the appendage is obtained from [13] as shown below in (14) and (15).

$$\emptyset_i(x) = C_n\begin{Bmatrix}(\cos\beta_n x - \cosh\beta_n x) \\ +\alpha(\sin\beta_n x - \sinh\beta_n x)\end{Bmatrix} \qquad (14)$$

Where,

$$\alpha = \frac{(\sin\beta_n L - \sinh\beta_n L)}{(\cos\beta_n L + \cosh\beta_n L)} \qquad (15)$$

The C_n represents the arbitrary constant and β_n is obtained from the assumed boundary condition of the deforming structure which is the solar panel. In this case, the boundary condition of the solar panel is a fixed-free configured beam and may be obtained through the following (16).

$$\cos\beta_n L + \cosh\beta_n L + 1 = 0 \qquad (16)$$

While, C_n can be obtained through normalization of the mode shape function to range between 0 to 1. Hence, C_n chosen must gives

$$\int_0^1 \left(\emptyset_i(x)\right)^2 dx = 1 \tag{17}$$

However, the mode shape function is orthogonal in the following condition

$$\int_0^1 \emptyset_i(x)\emptyset_j(x)dx = 0 \qquad \text{when } i \neq j \tag{18}$$

Incorporate the assumed equation, (13) into total kinetic energy and potential energy would yield (19) – (21).

$$T_\varphi = \frac{1}{2}I\dot{\varphi}^2 + \frac{1}{2}\int_0^{z_i}\int_{-\frac{w_i}{2}}^{\frac{w_{i1}}{2}}\int_0^{L_i}\sum_{i=1}^{3}\rho_i[B]\,dxdydz \tag{19}$$

Where,

$$B = \begin{bmatrix} \dot{\varphi}^2(c + z_i + q_i\emptyset_i)^2 \\ +\{y_i\dot{\varphi}\cos(D_i) + q_i\emptyset_i - (a+x)\dot{\varphi}\sin(D_i)\}^2 \end{bmatrix} \tag{20}$$

$$U_\varphi = \sum_{i=1}^{3}\int_0^{L_i} E_iI_i\ddot{\emptyset}_i{}^2 q_i{}^2 dx \tag{21}$$

From here, the final dynamics may be obtained by using the Lagrange Equation for four generalized coordinates represented by A_j (j=1,2,3,4), which are the angular rotation φ and elastic motion q_i for i=1,2,3 represented by the 3 solar panels.

$$\frac{d}{dt}\left(\frac{\partial T}{\partial \dot{A}_j}\right) - \frac{\partial T}{\partial A_j} + \frac{\partial U}{\partial A_j} = Q \tag{22}$$

Q represents the generalized forces of the system. Substitute (19) and (21) into (22) and the mathematical modal equation for the satellite for φ axis torque application is obtained.

$$\left\{\begin{array}{l}\left[I_\varphi + \int_0^{z_i}\int_{-\frac{w_i}{2}}^{\frac{w_i}{2}}\int_0^{L_i}\sum_{i=1}^{3}\rho_i[H_1]dxdydz\right]\ddot{\varphi} \\ +\sum_{i=1}^{3}\left[\rho_i\int_0^{z_i}\int_{-\frac{w_i}{2}}^{\frac{w_i}{2}}\int_0^{L_i}[H_2\}\,dxdydz\right]\ddot{q}_i\end{array}\right\} = \tau_\varphi \tag{23}$$

and

$$\sum_{i=1}^{3}\left\{\begin{array}{l}[H_2]\ddot{\varphi} \\ +[H_3]\ddot{q}_i \\ +[H_4]q_i\end{array}\right\} = 0 \tag{24}$$

where,

$$H_1 = \begin{bmatrix}(c + z_i + q_i\emptyset_i)^2 \\ +y_i{}^2\cos^2(D_i) \\ +(a+x)^2\sin^2(D_i)\end{bmatrix} \tag{25}$$

$$H_2 = y_i\cos(D_i)\,\emptyset_i - (a+x)\sin(D_i)\emptyset_i \tag{26}$$

$$H_3 = \rho_i\int_0^{z_i}\int_{-\frac{w_i}{2}}^{\frac{w_i}{2}}\int_0^{L_i}\emptyset_{ni}\emptyset_{mi}\,dx\,dy\,dz \tag{27}$$

$$H_4 = \begin{bmatrix}\int_0^{L_i} E_iI_i\ddot{\emptyset}_{ni}\ddot{\emptyset}_{mi}\,dx \\ -\rho_i\int_0^{z_i}\int_{-\frac{w_i}{2}}^{\frac{w_{i1}}{2}}\int_0^{L_i}\dot{\varphi}^2\emptyset_{ni}\emptyset_{mi}\,dx\,dy\,dz\end{bmatrix} \tag{28}$$

3.0 DYNAMIC SIMULATION

MATLAB toolbox, SIMULINK is chosen to perform the simulation on the model and ANSYS is used to verify the model. The simulation is done based on the assumption that there is no external disturbance existed, and that the attitude maneuvering is done on 1 axis at a time, while the other 2 axis remain constant. The initial condition for the satellite is assumed to be constant. The input of the torque application is an impulse signal that shows sudden disturbance in the system as shown in the Figure 6. The three solar panels appended to the rigid hub is identical, hence they inherent the similar specification.

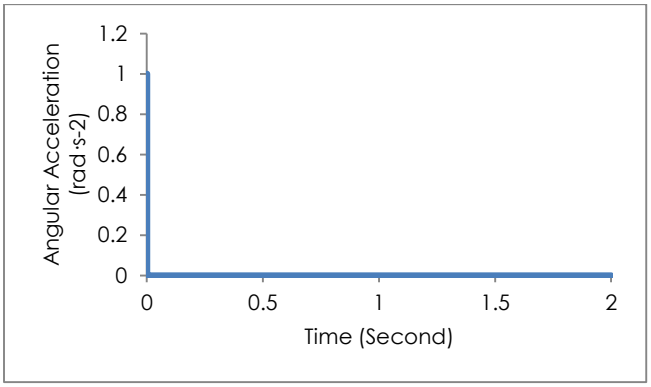

Figure 6 Impulse Input

The system parameters and maneuver specifications are listed in Table 1.

Table 1 System specification

Description	Symbol	Value
Length of the panel	L	0.818 m
Height of the panel	z	0.020 m
Width of the panel	W	0.567 m
Distance O to P (x axis)	A	0.491 m
Distance O to P (z axis)	C	0.456 m
Weight per unit volume of panel	P	1040 Kg/m^3
Young's Modulus of panel	E	3.6 GPa

The displacement on the tip of the flexible panels for panel 1, 2 and 3 due to the application of the input torque to the satellite models are illustrated in Figures. 7 and 8 since the response of panel 2 and 3 are identical.

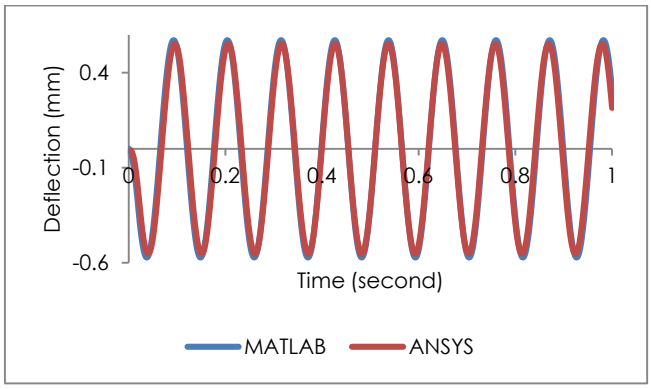

Figure 7 Tip displacement of Panel 1

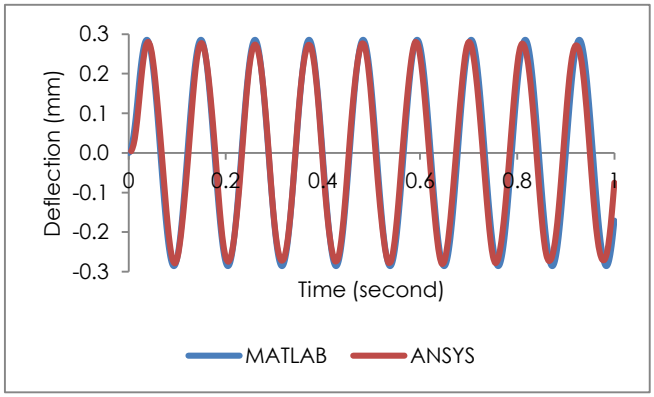

Figure 8 Tip displacement of Panel 2 and 3

As shown, the results from the satellite in Figures 7 and 8, the simulation of the MATLAB based on dynamic model and ANSYS which is based on finite element analysis are consistent with each other. Hence, the model is applicable on the basis that both simulation methods coincide with minor differences. However, further refinement of the dynamic to suit the actual physical world may be applied by including additional factors such as the axial deformation, vibration due to the centripetal effect and external interferences. Study on the impulse input onto the system is crucial as to determine the flexibility behavior of the system when exposed to such disturbances. Neglecting the damping effect, when the impulse torque is applied on the system, the flexible panels undergo a harmonic motion. These harmonic motion may seemed harmless to the system, but in reality, high precision is a must in space mission as every error that exists may pose hazard to the system itself. In the case of satellite imaging (as what RazakSAT® was build for), having these slight vibration may render the captured image useless ranging from image quality degradation [14].

4.0 MODAL ANALYSIS

The bending vibration of the satellite panels is governed by (24). The structure of the panel along the x axis remains constant. Hence, the equation may be rewritten in a dimensionless form. To achieve this, the following assumptions of dimensionless variables are introduced.

$$\tau = \frac{t}{T} \tag{29}$$

$$\xi = \frac{x}{L} \tag{30}$$

$$\mu = \frac{q}{L} \tag{31}$$

$$\gamma = T\dot{\varphi} \tag{32}$$

where T is obtain as follow [15],

$$T = \frac{\rho L^4}{EI} \tag{33}$$

Incorporating these equations into (24) while neglecting the input torque, one obtain,

$$M\ddot{\mu} + K\mu = 0 \tag{34}$$

Where the two dots over the μ is the double differential of μ with respect to non-dimensional time, τ and

$$M = \int_0^1 \zeta_{mi}\zeta_{ni}d\xi \tag{35}$$

$$K = \int_0^1 \zeta_{mi,\xi\xi}\zeta_{ni,\xi\xi}d\xi - \gamma^2 \int_0^1 \zeta_{mi}\zeta_{ni}\,dx \tag{36}$$

Where ζ_{mi} is a function of ξ and is similar to the function ϕ_{mi}. Hence, From equation (34), an eigenvalue problem for the bending vibration of a the solar panel can be formulated by assuming that the μ is harmonic.

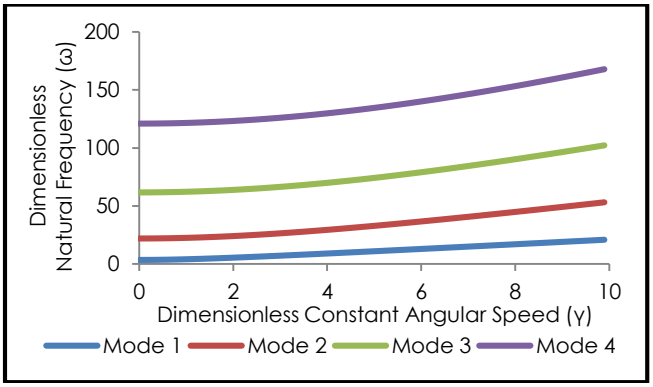

Figure 9 Natural frequency variation

The variations of natural frequency due to the different angular velocity are shown in Figure 9. The lowest four vibration modes are plotted. Observable from the figure, the dimensionless natural frequencies increase as the constant dimensionless angular speed is increased. As the dimensionless angular speed increases, the slope of the trajectory becomes steeper in an exponential form. Avoiding torque that is capable of generating frequency similar to the natural frequency is important to avoid large amplitude harmonic motion that may disorientated and disrupt the satellite system.

5.0 CONCLUSION

A dynamic equation of a RazakSAT® class satellite three flexible solar panels for three-dimensional dynamic studies is developed based on the coupling deformation field. A comprehensive model of the flexible satellite considering solar panels as flexible, finite element panels is provided in an ANSYS environment as reference when comparing the dynamic models. However in slight differences between the two simulations provides a room for further refinement of the dynamic model such as the stiffening of the panels due to the centrifugal force due to the fact that the panels are appended with an offset to the axis of rotation.

References

[1] R. E. Roberson. 1979. Two Decades of Spacecraft Attitude Control. *Journal of Guidance, Control, and Dynamics*. 2(1): 3-8.

[2] J. L. Junkins. 1997. Adventures on the Interface of Dynamics and Control. *Journal of Guidance, Control, and Dynamics*. 20(6): 1058-1071.

[3] V. J. Modi. 1974. Attitude Dynamics of Satellites with Flexible Appendages-A Brief Review. *Journal of Spacecraft and Rockets*. 11(11): 743-751.

[4] Y. Zeng, A. D. Araujo and S. N. Singh. 1999. Output Feedback Variable Structure Adaptive Control of Flexible Spacecraft. *Acta Astronautica*. 44(1): 11-22.

[5] H. Bang, Y. Cho and H. Lee. 2004. Slewing Maneuver Control of Flexible Spacecraft by Output Feedback. *Acta Astronautica.* 55: 903-916.

[6] Q. Hu and G. Ma. 2005. Variable Structure Control and Active Vibra-Tion Suppression of Flexible Spacecraft During Attitude Maneuver. *Aerospace Science and Technology*. 307-317.

[7] Q. Hu and Y. Liu. 2005. A Hybrid Scheme of Feed-Forward/Feed-Back Control for Vibration Suppression of Flexible Spacecraft with On-Off Actuators During Attitude Maneuver. *International Journal of Information Technology*. 11(12): 95-107.

[8] B. N. Agrawal, R. S. Mcclelland and G. Song. 1997. Attitude Control of Flexible Spacecraft Using Pulse-width Pulse-Frequency Modulation Thrusters. *Space Technology*. 17(1): 15-34.

[9] G. Song and B. N. Agrawal. 2001. Vibration Suppression of Flexible Spacecraft During Attitude Control. *Acta Astronautica.* 49(2): 73-83.

[10] J. Liu and J. Hong. 2004. Geometric Stiffening Effect on Rigid-Flexible Coupling Dynamics of an Elastic Beam. *Journal of Sound and Vibration*. 278(4): 1147-1162.

[11] J. Hong and C. You. 2004. Advances in Dynamics of Rigid-Flexible Coupling System. *Journal of Dynamics and Control.* 2(2): 1-6.

[12] H. Yang, J. Hong, and Z. Yu. 2003. Dynamics Modeling of a Flexible Hub-beam System with a Tip Mass. *Journal of Sound and Vibration.* 266(4): 759-774.

[13] Meirovitch L. 1968. *Elemenrs of Vibration Analysis.* McGrawHill Company.

[14] Wang Zhi-le, Li Bo, Zhang Yuan, Xiao Hao-su, Zhou Cheng-hao. 2012. Satellite Vibration on Image Quality Degradation of Remote Sensing Camera. *Research on Precision Instrument and Machinery (RPIM)*. 1(1): 6-10.

[15] H. H. Yoo and S. H. Shin. 1998. Vibration Analysis of Rotating Cantilever Beam. *Journal of Sound and Vibration*. 221(5): 807-828.